On the probability of ventricular fibrillation due to electric shock

G. Pritchard[1] G. C. Livingston Jr[2] R. Aggarwal[3]
I. Griffiths[4] H. Waterer[5] M. H. Meylan[6]
J. Juniper[7]

(Received 2 November 2020; revised 21 June 2022)

Abstract

When exposed to a specified electrical shock, the probability that a randomly chosen individual will undergo fatal ventricular fibrillation can be regarded as a function of random variation in the human population along two dimensions. The first dimension is the individual's body impedance characteristic: for this, we introduce a new two-parameter model that improves on the simpler one-parameter model used in previous work. The second dimension is the individual's current tolerance: we codify some curves used in previous practice. We also consider methods of solving the resulting shock circuit and show that the fixed-point iteration method can give incorrect results.

DOI:10.21914/anziamj.v62.15969, Published 2022-07-16, as part of the Proceedings of the 2020 Mathematics and Statistics in Industry Study Group. ISSN 1445-8810. (Print two pages per sheet of paper.)

Contents

1 Introduction M66

2 The rate of shocks M67

3 Modelling the human body impedance M71

4 Solving the shock circuit M77

5 The human current tolerance M80

6 The probability of ventricular fibrillation M82

7 Conclusion M85

1 Introduction

The statistical modelling of electrical shock hazards is both decades old (Wang et al. 1984) and still of current interest (Dimopoulos et al. 2012; Griffiths and Woodhouse 2017). While there are several possible approaches, there is general agreement that a key concept is that of the *ventricular fibrillation probability*. This is the probability that an individual randomly chosen from the population will undergo ventricular fibrillation leading to death when subjected to electrical shock of a specified kind. It is generally accepted that ventricular fibrillation is the principal cause of fatalities due to electrical shock.

The fibrillation-probability problem decomposes into two parts. Firstly, fibrillation is triggered by an electrical current passing through the heart, but the threshold amount of current required to cause fibrillation (called the *current tolerance*) varies among individuals, and so a statistical approach is called for. Secondly, the amount of current that flows through the body depends on the *body impedance*, which varies nonlinearly with the voltage across the body

(called the *touch voltage*) and also among individuals. We must thus consider random variation in the human population under consideration along two dimensions: current tolerance and body impedance. The statistical problem is then one of estimating a bivariate probability distribution and the fibrillation probability P_{fib} a bivariate expectation.

This two-variable paradigm, although very useful, is complicated somewhat by the fact that body impedance is a function (of the touch voltage) rather than a single variable. The simplest body impedance models remove this complication by modelling body impedance functions as a one-parameter family—but this introduces some undesirable non-monotone behaviour. One of this paper's principal original contributions is a new two-parameter model that preserves monotonicity with voltage; this is the subject of Section 3.

A further complication is that for engineering calculations, the fibrillation probability is rarely interesting in itself: what the engineer wants to know is whether a particular piece of equipment will cause fatalities by electrocution at an acceptably low rate. This requires an additional model of the rate λ_{s} (per unit time) at which shocks—opportunities for current to flow through the bodies of unfortunate humans—will occur. The probability that a shock results in a fatality is identified with the fibrillation probability. The long-run average rate of fatalities is then $\lambda_{\text{s}}\mathsf{P}_{\text{fib}}$ per unit time. This wider view of the problem is developed in Sections 4 to 6.

The Australian industry-standard (but closed-source) software known as *Argon* performs calculations similar to ours. This paper examines the standard underpinning the Argon software suite and replicates, evaluates, and improves on the approach adopted therein.

2 The rate of shocks

The occurrence of shocks is modelled in the following simple way. A given piece of equipment is assumed to experience faults from time to time at

Figure 1: The fault and contact processes.

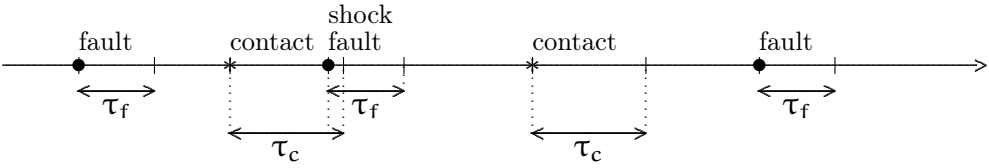

random. We model these faults as a Poisson point process in time with a given rate of λ_f faults per unit time. Every fault is assumed to have a given duration τ_f. Without loss of generality, we suppose that an event of the Poisson process at time t marks the beginning of the corresponding fault period, so that the fault lasts for the time interval $[t, t+\tau_f]$ (Figure 1). During a fault, some surfaces that are accessible to humans become electrically live.

Actual contact between humans and potentially dangerous surfaces occurs from time to time in a way that we also model as a Poisson process, with rate λ_c contacts per unit time. Every contact is assumed to have a given duration τ_c. Again without loss of generality, we suppose that an event of the Poisson process at time s marks the beginning of the corresponding contact period, so that the contact exists during the time interval $[s, s+\tau_c]$. The fault and contact processes are assumed independent.

A shock occurs when a fault overlaps in time with a contact (a "coincidence"). The rate of coincidences, per unit time, is derived in the following way. Suppose a fault exists during the time interval $[t, t+\tau_f]$. A contact existing during the time interval $[s, s+\tau_c]$ creates a coincidence—that is, the intervals overlap—if, and only if, $t-\tau_c < s < t+\tau_f$. The fault is thus associated with a time interval $[t-\tau_c, t+\tau_f]$ during which the initiation of any contact causes a coincidence. Since the length of this interval is $\tau_f + \tau_c$, the number of coincidences arising from it has a Poisson distribution with mean $\lambda_c(\tau_f + \tau_c)$.

Now consider a time interval $[0, T]$, during which faults are initiated at times $T_1, \ldots, T_N$. By assumption, N has a Poisson distribution with mean $\lambda_f T$.

The total number of coincidences is $X = \sum_{i=1}^{N} X_i$, where X_i is the number of coincidences associated with the fault that exists during the time interval $[T_i, T_i + \tau_f]$. Hence,

$$E[X] = E\left[\sum_{i=1}^{N} X_i\right] = E[N]E[X_1] = \lambda_f T \cdot \lambda_c(\tau_f + \tau_c).$$

Therefore, the rate of coincidences (or shocks) is $\lambda_s = \lambda_f \lambda_c(\tau_f + \tau_c)$ per unit time.

The preceding analysis takes no account of the possibility of faults coinciding with each other; similarly contacts. Should two faults overlap in time, they are counted as separate events, and any coincidences they give rise to are counted separately. Similarly, the exceptionally unlucky individual whose contact period overlaps with two distinct faults (which may or may not overlap with each other) is considered to have experienced two coincidences and been exposed to two shock hazards. While the realism of this neglect may be problematic, the effect on the results should be small, provided that faults and contacts are both rare events.

This analysis differs somewhat from a slightly different approach by Pawlik, Griffiths, and Woodhouse (2018), which involves a detailed calculation of the *probability of at least one* coincidence occurring during a given time interval. The analysis in this paper instead tells us the *expected number* of coincidences during the time interval. The two values will be very similar if coincidences are rare enough to make it very unlikely that two or more occur during the interval. However, the latter approach is better suited to our purposes, as the expected number of coincidences can be multiplied by a fibrillation probability to obtain the expected number of fatalities.

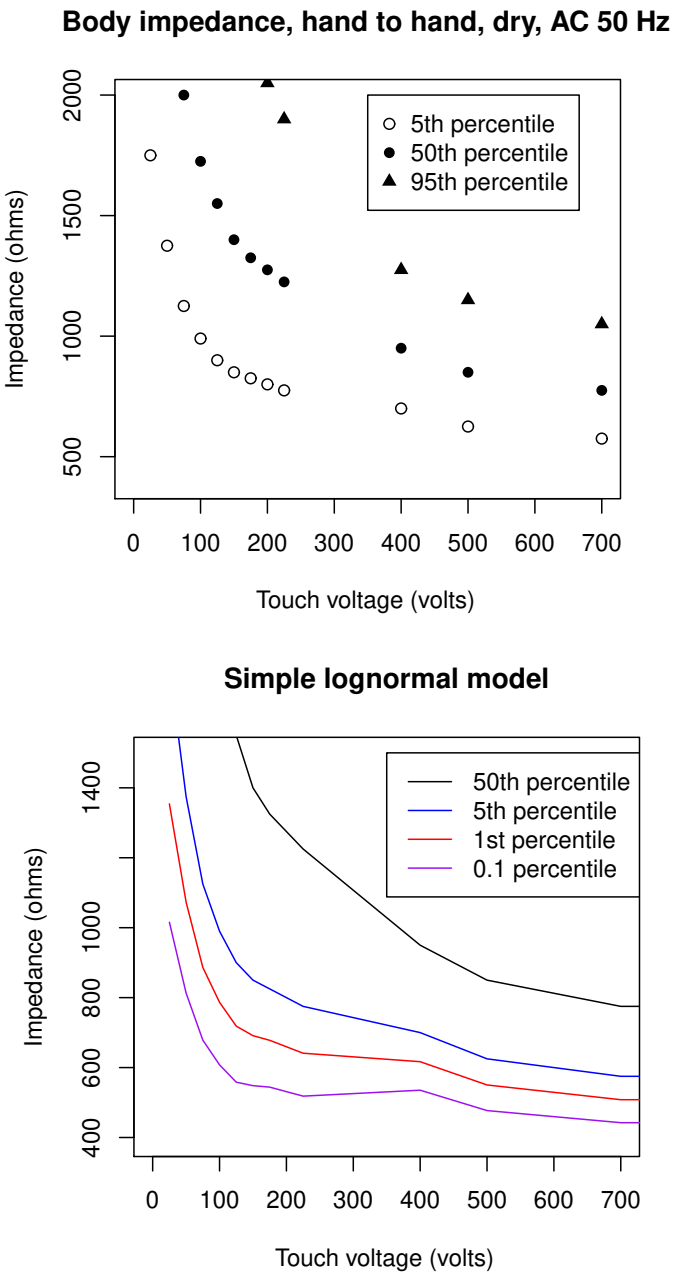

Figure 2: (top) body impedance data (International Electrotechnical Commission 2018); and (bottom) a simple lognormal fit.

Table 1: Body impedance statistics at various voltages (hand-to-hand, dry, large contact area, AC 50–60 Hz) (International Electrotechnical Commission 2018).

Voltage (V)	Impedance (Ω) 5th percentile	50th percentile	One-parameter model mean(log)	sd(log)	Two-parameter model β
25	1750	3250	8.086	0.376	1.000
50	1375	2500	7.824	0.363	0.735
75	1125	2000	7.601	0.350	0.523
100	990	1725	7.453	0.338	0.413
125	900	1550	7.346	0.330	0.339
150	850	1400	7.244	0.303	0.280
175	825	1325	7.189	0.288	0.250
200	800	1275	7.151	0.283	0.229
225	775	1225	7.111	0.278	0.209
400	700	950	6.856	0.186	0.106
500	625	850	6.745	0.187	0.067
700	575	775	6.653	0.181	0.040
1000	575	775	6.653	0.181	0.040

3 Modelling the human body impedance

The starting point for this section of the paper is available data on human body impedance published by International Electrotechnical Commission (2018) and AS/NZS 60479.1 (2010). Estimates are tabulated of the 5th, 50th, and 95th percentiles of the impedance at a finite set of voltages ranging from 25 V to 1000 V; the first two of these quantiles are reproduced in Table 1. Similar tables are available for other current paths (e.g., left-hand-to-right-foot, or foot-to-foot) and for contact made with wet or saltwater-wet skin. The data are illustrated in Figure 2 (left).

The body impedance is principally resistive. Although the skin exhibits some

capacitive behaviour, this is relatively small (International Electrotechnical Commission 2018) and we neglect it: references in this paper to "impedance" are to resistance only.

A simple modelling approach (Griffiths and Woodhouse 2017) is to fit a lognormal distribution to the given quantiles for each given voltage. This choice of distribution is suggested by data (Biegelmeier 1979); it also has the desirable feature that it guarantees non-negativity. The lognormal distribution, which has two parameters, is fit exactly to the given values for the 5th and 50th percentiles. The 95th percentile value is regarded as being of less interest for present purposes—it is the individuals with low body impedance who carry the highest currents and so are most likely to perish from electric shock—although it is reproduced quite well by the fitted lognormal distributions. Fitted parameters (mean and standard deviation of the log(impedance)) are recorded alongside the data in Table 1.

To model the body impedance characteristics of individuals, we need a further assumption regarding the correlation between impedances at different voltages. The simplest thing is to posit a perfect correlation: each individual's body impedance coincides with the same population quantile at all voltages. So, for example, an individual whose body impedance at 25 V happens to match the population median has a body impedance at 1000 V matching the population median for that statistic also. The body impedance functions of the human population are thus modelled as a one-parameter family: any individual's body impedance is completely specified, as a function of voltage, by the population quantile with which the individual coincides.

This simple lognormal model is used to extrapolate the impedance distributions to lower quantiles, as shown in Figure 2 (right). Doing so reveals the main flaw in this approach: the impedance is no longer a monotone function of voltage for the most extreme quantiles. This is unappealing because we expect on physical grounds that the impedance characteristic of any individual is monotone decreasing in voltage; therefore, any quantile of the population should be monotone decreasing also.

It is readily apparent why the simple lognormal model fails in this way: the impedance (or rather, its logarithm) at low voltages has greater variance than at high voltages. Suppose we have voltages $V_1 < V_2$ with the log(impedance) at voltage V_i $(i = 1, 2)$ having mean μ_i and variance σ_i^2. Then the α-quantile of the log(impedance) at V_i is $\mu_i + \sigma_i q_\alpha$, where q_α is the α-quantile of the standard normal distribution. If $\mu_1 > \mu_2$ (as we expect), but also $\sigma_1 > \sigma_2$, then for $q_\alpha < \frac{\mu_2 - \mu_1}{\sigma_1 - \sigma_2}$ we have $\mu_1 + \sigma_1 q_\alpha < \mu_2 + \sigma_2 q_\alpha$. That is, for sufficiently extreme quantiles in the left tail of the distributions, the low-voltage impedance falls below the high-voltage impedance.

The physical basis for the voltage-dependence of the body impedance lies in the behaviour of the skin, which presents a relatively large impedance to low voltages. Still, it breaks down for voltages on the order of a few hundred volts. This points the way towards an improved model: the skin and the subdermal tissue are treated separately:

$$Z_b(V) = Z_{skin}\ \beta(V)\ +\ Z_{subd}. \tag{1}$$

That is, the body impedance function of any individual is the sum of two terms, representing skin and subdermal impedances in series. Only the skin impedance is voltage-dependent. The body impedance functions of the human population are thus modelled as a two-parameter family: each individual has their own values for the two parameters Z_{skin} and Z_{subd} whereas $\beta(V)$ is a fixed function common to all individuals. We assume that Z_{skin} and Z_{subd}, which we must now regard as random variables, are independent and both log-normally distributed.

The impedance curves of two different individuals may cross, something not possible with the simple lognormal model. The impedance function of any individual is guaranteed to be decreasing with voltage (provided the function β is decreasing).

Another point in favour of the model (1) is that it has fewer parameters than the simpler lognormal model. Suppose the model must predict the impedance

at voltages $V_1, \ldots, V_n$. The simple lognormal model requires $2n$ parameters: a mean and variance for each voltage. But (1) requires only $n+3$ parameters: two each for the distributions of Z_{skin} and Z_{subd}, and $n-1$ for the values of $\beta(V_2), \ldots, \beta(V_n)$. (Without loss of generality, we take $\beta(V_1) = 1$ for the smallest voltage V_1.) We denote this parameter vector by θ.

We again fit the model (1) to the tabulated 5th and 50th percentile impedance values at the voltages $V_1, \ldots, V_n$. These quantiles, which we denote $q_5^1, \ldots, q_5^n$ and $q_{50}^1, \ldots, q_{50}^n$, are themselves summary statistics of an underlying sample, which is inaccessible to us. (We do not even know the sample size, a shortcoming with implications we return to in the final paragraph of this section). Our knowledge of the sample data at voltage V_i is limited to the information that 5% of the values are less than q_5^i, 45% are between q_5^i and q_{50}^i, and 50% exceed q_{50}^i.

We take a maximum-likelihood approach to the fitting. Assuming a model that gives a cumulative distribution function $F_i(\cdot; \theta)$ for the impedance at V_i, the likelihood of the observed values at this voltage is

$$F_i(q_5^i; \theta)^{0.05N} \cdot \left[F_i(q_{50}^i; \theta) - F_i(q_5^i; \theta)\right]^{0.45N} \cdot \left[1 - F_i(q_{50}^i; \theta)\right]^{0.5N},$$

where N is the unknown sample size. Hence, the log-likelihood function for the full dataset is

$$\theta \mapsto N \sum_{i=1}^{n} \left\{0.05 \log F_i(q_5^i; \theta) + 0.45 \log(F_i(q_{50}^i; \theta) - F_i(q_5^i; \theta)) + 0.5 \log\left[1 - F_i(q_{50}^i; \theta)\right]\right\}. \tag{2}$$

In summing log-likelihoods across voltages we make the implicit assumption of independence between voltages. This assumption is problematic because the original data were likely obtained by making measurements at several voltages on each test subject. It is not necessary to know the value of N to maximize (2) over θ.

In the particular case of interest here, we have $n = 13$ different voltages. The parameter vector θ is of size 16:

$$\theta = (\mu_{\text{skin}}, \sigma_{\text{skin}}, \mu_{\text{subd}}, \sigma_{\text{subd}}, \beta_2, \ldots, \beta_n)$$

where μ_{skin} and σ_{skin} are the mean and standard deviation of $\log Z_{\text{skin}}$; similarly μ_{subd}, σ_{subd}; and $\beta_2, \ldots, \beta_n$ are the values of $\beta(V_2), \ldots, \beta(V_n)$.

In carrying out this nonlinear optimization, we have the difficulty that for a given θ, the distribution $F_i(\cdot; \theta)$ is that of the sum of two independent lognormally-distributed random variables, and so there is no closed-form analytical expression for $F_i(q; \theta)$ as a function of θ. We overcome this problem by Monte Carlo sampling, in the following way. First, draw large independent random samples $(W_k^{\text{skin}})_{k=1}^M$ and $(W_k^{\text{subd}})_{k=1}^M$ according to the standard normal distribution; we used $M = 10^5$. These samples, once drawn, remain fixed throughout the fitting. Then for any θ, $(Z_{ki})_{k=1}^M$ defined by

$$Z_{ki} = \exp\left(\mu_{\text{skin}} + \sigma_{\text{skin}} W_k^{\text{skin}}\right) \beta_i + \exp\left(\mu_{\text{subd}} + \sigma_{\text{skin}} W_k^{\text{subd}}\right)$$

is an independent random sample drawn according to the distribution of body impedances at voltage V_i ($i = 1, \ldots, n$) corresponding to θ. We use the proportion of values in this sample that are less than q as an approximation to $F(q; \theta)$.

Fitted values of the $\beta(V_i)$ parameters are recorded alongside the data in Table 1. The corresponding fitted distributional parameters for $\log(Z_{\text{skin}})$ are $\mu_{\text{skin}} = 7.84$ and $\sigma_{\text{skin}} = 0.62$; those for $\log(Z_{\text{subd}})$ are $\mu_{\text{subd}} = 6.49$ and $\sigma_{\text{subd}} = 0.19$. Figure 3 illustrates the model obtained. A good fit is achieved to the required 5th and 50th percentile values. The extrapolated 1st percentile and 0.1 percentile curves are monotone decreasing as expected, and for high voltages are in good agreement with those extrapolated by the simple lognormal model. (This, too, is expected since the skin term becomes negligible at high voltages). The models differ most at around 200 V. Figure 3 (right) shows that it is not only possible but quite common for the impedance characteristics of different individuals to cross: one individual may have

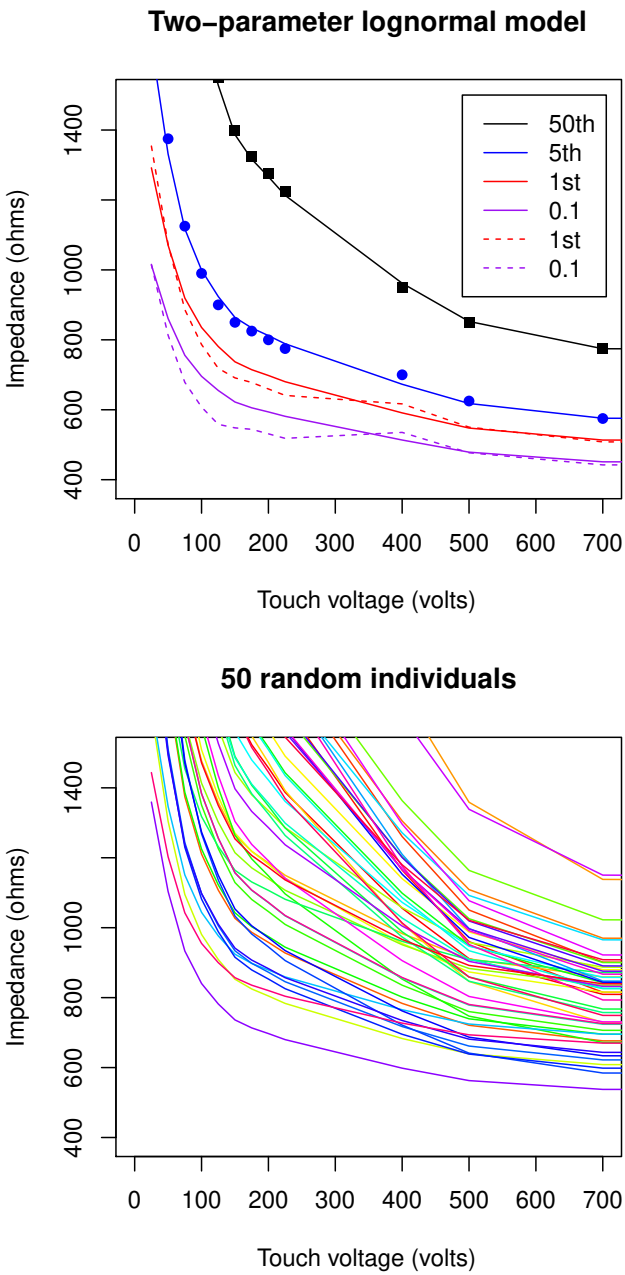

Figure 3: The two-parameter model of body impedance: (top) percentiles, with raw data plotted as points and the curves of Figure 2 reproduced as dotted lines; and (bottom) 50 randomly sampled individuals.

relatively high-impedance skin and a low-impedance internal body, whereas another has low-impedance skin and a high-impedance internal body.

It would be desirable to quantify the uncertainty in the estimates of the model parameters for both the simple lognormal model and our two-parameter model. Unfortunately, the nature of the available data makes this impossible. The parameter uncertainties depend on the uncertainties in the published quantiles in Table 1, which themselves depend mainly on the size of the underlying sample. But the International Electrotechnical Commission (2018) does not make this information available.

4 Solving the shock circuit

In this section we consider the shock circuit comprising a voltage source connected across two impedances in series, one of which is a human body. The other impedance—which may represent footwear, gloves, soil, paving material, etc.—is assumed (as with the body impedance) to be purely resistive and to have a fixed value Z_s. The source voltage (also known as the *prospective touch voltage*) is denoted V_s.

As discussed in Section 3, the impedance of the human body is voltage-dependent; we denote it $Z_b(V)$ at voltage V, and define this quantity for all voltages V by linear interpolation between the tabulated voltages $V_1, \ldots, V_n$. For completeness, we define $Z_b(V) = Z_b(V_1)$ for $0 \leqslant V < V_1$ and $Z_b(V) = Z_b(V_n)$ for $V > V_n$. (The first of these approximations has poor accuracy, but this is not a concern as the very lowest voltages and highest impedances are not hazardous in any case.)

The voltage across the body (known as the *touch voltage*) V_t then satisfies

$$V_t = \frac{Z_b(V_t)}{Z_s + Z_b(V_t)} V_s \tag{3}$$

or equivalently

$$Z_b(V_t) - \frac{Z_s V_t}{V_s - V_t} = 0. \tag{4}$$

Provided Z_b is a decreasing function, there exists a unique solution to (4) with $0 < V_t < V_s$, since the left-hand-side of (4) is a strictly decreasing continuous function of V_t on that interval which takes positive values as $V_t \to 0$ and negative values as $V_t \to V_s$.

Section 3 shows that the simple lognormal model may have some quantiles which are not decreasing functions of the voltage, creating the mathematical possibility of multiple solutions to (4). However, such cases are found to exist only for very extreme quantiles corresponding to a fraction circa 10^{-20} (or less) of the population, and we do not consider them further.

Equation (3) could be solved by fixed-point iteration (Griffiths and Woodhouse 2017) on the function $f(v) = V_s Z_b(v)/[Z_s + Z_b(v)]$. That is, a sequence $(v_k)_{k=0}^{\infty}$ is defined by letting $v_0 = V_s$ and $v_k = f(v_{k-1})$ for $k = 1, 2, \ldots$. In cases of practical interest, this sequence always seems to converge to the solution of the equation. However, fixed-point iteration is well-known to be a method that works in some situations but not in others, and in some (relatively rare) cases this approach to solving (3) may fail.

Example Let $Z_s = 10\,\mathrm{k\Omega}$ and $V_s = 3200\,\mathrm{V}$, and let the exposed individual have a body impedance coinciding with the 98th percentile of the population according to the simple lognormal model given in Section 3. According to this model, the body impedances are $2170\,\Omega$, $1391\,\Omega$, and $1248\,\Omega$ at $225\,\mathrm{V}$, $400\,\mathrm{V}$, and $500\,\mathrm{V}$, respectively. Solving (3) reveals the touch voltage to be $V_t = 395.59\,\mathrm{V}$, with the corresponding body impedance being $1410.6\,\Omega$ and body current $280\,\mathrm{mA}$. However, if the above fixed-point iteration is initiated from $395\,\mathrm{V}$ (or any close approximation of the solution) it will not converge to the correct value, but will eventually alternate between values $390.26\,\mathrm{V}$ and $401.4\,\mathrm{V}$, which constitute a two-cycle for f.

Figure 4: Human current tolerance diagram, reproduced from the International Electrotechnical Commission (2018).

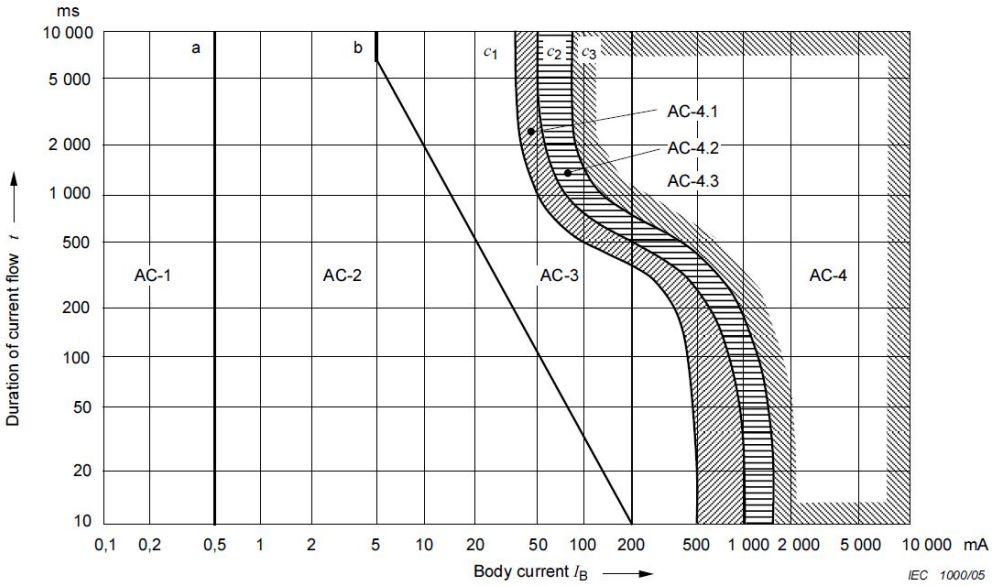

In general, a necessary condition for the successful convergence of the fixed-point iteration is $|f'(V_t)| \leqslant 1$ (Burden and Faires 2001; Hoffman 2001). We have

$$f'(v) = \frac{V_s Z_s Z_b'(v)}{(Z_s + Z_b(v))^2},$$

which for the above numerical example gives $f'(V_t) \approx -1.09$.

An alternative and more reliable method of solving (3) is a simple bisection search for the touch voltage V_t satisfying (4); this method is used for calculations in this paper.

5 The human current tolerance

The foregoing sections have been concerned with models predicting electrical current through the body: how much current flows, and how often? In this section we turn our attention to the other key variable in the fibrillation-probability problem: the ability of individuals to tolerate current through the body without triggering ventricular fibrillation and death.

As with most published work in this area, we begin with the diagram in Figure 4 (International Electrotechnical Commission 2018; Biegelmeier 1987; Biegelmeier 1960). The current tolerance depends on the duration of the exposure: short electric shocks are less harmful than prolonged ones. Of interest are the three S-curves in Figure 4, which represent thresholds at which ventricular fibrillation occurs with probabilities of 5%, 50%, and 95%.

We do not propose, in this paper, to modify or re-model these curves, but only to render them into a numerical form suitable for computation. Two curve-fitting approaches were trialled: one a generalized logistic function fitted with ceiling, floor and growth rate estimated by minimizing the root mean squared error, the other a polynomial spline. Comparison of the residuals suggests that the spline approach is favoured over the logistic estimate (and results did not seem to vary much on a substantive basis when the number of steps chosen for fitting the spline were increased from 13 to 113).

A univariate piecewise polynomial (pp) is specified by its break sequence `breaks` and the coefficient array `coefs` of the local power form of its polynomial pieces. The ppform of a polynomial spline of order k provides a description in the terms of the break points $\psi_1, \psi_2, \psi_3, \ldots, \psi_l + 1$ and the local polynomial coefficients C_{ji} of its l pieces:

$$P_j(x) = \sum_{i=1}^{k} (x - \psi_j)^{k-i} C_{ji}\,, \quad j = 1, \ldots, l\,. \tag{5}$$

We use a cubic spline: the order is $k = 4$. The break sequence is assumed

Figure 5: Spline curve fitted to the current-tolerance thresholds.

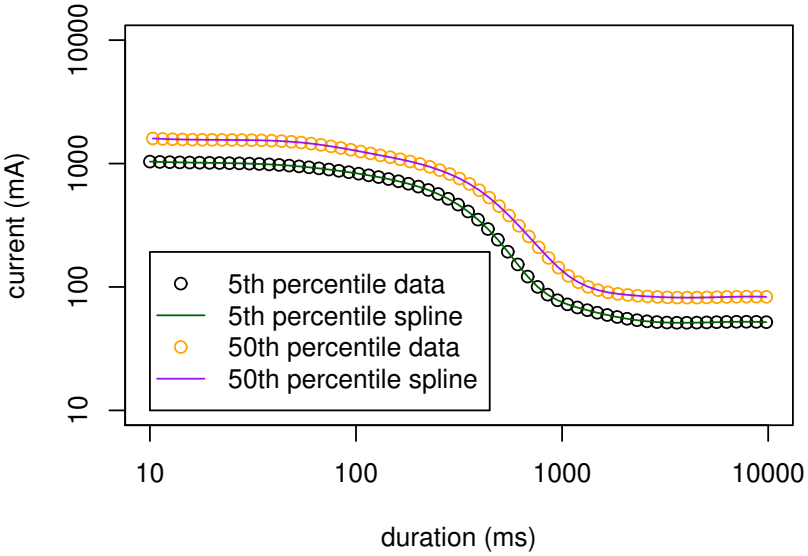

to be strictly increasing with l polynomial pieces that make up the ppform. The resulting interpolation is depicted in Figure 5.

The current tolerance, or threshold of ventricular fibrillation, varies among individuals, and so must be regarded as a random variable. Unlike the body impedance, it is a univariate random quantity. (As noted above, the current tolerance is also a function of the duration of exposure, but in most engineering calculations, the exposure time is regarded as a known constant.)

We regard each horizontal line in Figure 4 as a representation of the current tolerance distribution for a given duration. The points where the three S-curves in the figure cross the chosen horizontal line are the distribution's 5th, 50th, and 95th percentiles. No other information about the distribution is encoded in the figure.

Some further information about the distribution is available from animal

experiments (Biegelmeier and Lee 1980). A lognormal distribution has approximately the right shape, although it is not the only possibility.[1] This paper will use a lognormal distribution for current tolerance.

The curves in Figure 4, and their spline representations, give only the 5th, 50th, and 95th percentiles of the distribution. We take the straightforward approach of fitting a two-parameter lognormal distribution exactly to the required 5th and 50th percentiles of the distribution; it is then possible to calculate any desired quantile. Alternatively (and equivalently), it is possible to calculate the probability of fibrillation for a given current and exposure time.

As a numerical example, consider shocks whose duration is 1 second. According to Figure 4 (or more precisely, the spline approximations to the curves thereon), the 5th and 50th percentiles of the current tolerance at this duration are 50 mA and 78 mA respectively. The lognormal distribution with these quantiles gives the log(current) a mean value of $\log(78) \approx 4.36$ and standard deviation 0.27. The 95th percentile of this distribution is 122 mA (slightly below the spline-approximant value of 131 mA), and the fibrillation probability for a 100 mA shock is predicted to be 0.82.

6 The probability of ventricular fibrillation

A fundamental modelling assumption is that the body impedance curve and the current tolerance are statistically independent. This assumption seems to be made everywhere Energy Networks Association 2010, e.g. where both variables are considered, although it is far from clear that it is justified. For example, some association is found between an animal's body weight and its current tolerance (Ferris et al. 1936); it is easily imaginable that an individual's body weight or size will also affect the body impedance.

[1] Others include a three-parameter variant of the lognormal distribution (King and Coggan 2016), the normal distribution, or log-triangular distributions (Griffiths, Woodhouse, and Palmer 2013).

Suppose that the body impedance curve and the current tolerance are independent random quantities. On this assumption, it is in principle straightforward to calculate the probability of ventricular fibrillation resulting from a given shock. Denote by I the corresponding (random) body current: this depends only on the body impedance curve. Adopt a lognormal model for the current tolerance as suggested in Section 5, with log(current tolerance) having mean μ_f and standard deviation σ_f. Then, for a given I, the fibrillation probability

$$\Pr(\text{fibrillation} \mid I) = \Phi\left(\frac{\log I - \mu_f}{\sigma_f}\right),$$

where Φ denotes the standard normal cumulative distribution function. The unconditional fibrillation probability

$$\Pr(\text{fibrillation}) = \mathsf{E}\left[\Pr(\text{fibrillation} \mid I)\right] = \mathsf{E}\left[\Phi\left(\frac{\log I - \mu_f}{\sigma_f}\right)\right]. \tag{6}$$

Since I is a function of the body impedance curve only, we have an expectation of a function of this random curve.

For the simple lognormal model of body impedance, a random individual's body impedance curve is drawn from a one-parameter family: the sole parameter p (with $0 < p < 1$) specifies that the body impedance curve of the individual in question matches the population's p-quantile curve. The resulting current in the shock circuit is then a function of p; we denote it $g_1(p)$, so that (6) becomes

$$\Pr(\text{fibrillation}) = \int_0^1 \Phi\left(\frac{\log g_1(p) - \mu_f}{\sigma_f}\right) \mathrm{d}p\,. \tag{7}$$

That is, the required probability is obtained as a univariate integral. Even though the integrand is somewhat complicated—to evaluate it for a single value of p requires solving the shock circuit as described in Section 4—it is a simple matter to numerically evaluate such an integral (Griffiths and Woodhouse 2017).

For our two-parameter model of body impedance, a random individual's body impedance curve is given by (1); the parameters Z_{skin} and Z_{subd} appearing there are independent lognormally-distributed random variables. The resulting current is a function of these two parameters only: $I = g_2(Z_{skin}, Z_{subd})$. Hence

$$\Pr(\text{fibrillation}) = E\left[\Phi\left(\frac{\log g_2(Z_{skin}, Z_{subd}) - \mu_f}{\sigma_f}\right)\right]$$

or equivalently

$$\Pr(\text{fibrillation}) = E\left[\Phi\left(\frac{\log g_2(e^{\mu_{skin}+\sigma_{skin}W_1}, e^{\mu_{subd}+\sigma_{subd}W_2}) - \mu_f}{\sigma_f}\right)\right],$$

where W_1 and W_2 are independent standard normal random variables. It would be possible to express this expectation as a double integral, analogously to (7), but we do not pursue that approach here. Instead, we content ourselves with simple Monte Carlo simulations to evaluate the fibrillation probabilities.

Example A given item of equipment produces shocks by fault-contact coincidences at rate $\lambda_s = 0.01$ per annum—that is, the shocks are 1-in-100 year events. All the shocks are assumed to have duration 500 ms and protective series impedance $Z_s = 1\,k\Omega$. What is the maximum prospective touch voltage consistent with a fatality rate of 10^{-6} per annum?

The given rates imply that the fibrillation probability must be $P_{fib} = 10^{-4}$. Figure 4 indicates that for shocks of this duration, the current tolerance is 200 mA at the population median and half of this value at the 5th percentile; a lognormal model of current tolerance thus has mean (log current) equal to $\mu_f = \log(200)$ and standard deviation (log current) equal to $\sigma_f = \log(0.5)/\Phi^{-1}(0.05) = 0.421$. Using Monte Carlo samples of $n = 10^5$ body impedance curves suggests that the required prospective touch voltage may be taken to be 110 V; for this value of V_s, the estimated P_{fib} is $(93.1 \pm 1.3) \times 10^{-6}$ for the simple lognormal model of body impedance, and $(96.3 \pm 1.2) \times 10^{-6}$ for the two-parameter model.

7 Conclusion

As in earlier work, this paper decomposes the fibrillation-probability problem into two parts: individuals are assumed to vary both in their current tolerance and their body impedance characteristic. This decomposition reduces the problem to one of calculating a bivariate expectation. Body impedance is the more complicated variable, and for this we devise a new two-parameter model that may be more realistic than the simpler model previously used.

We also follow the approach of explicitly allowing for a series impedance in the circuit (Griffiths and Woodhouse 2017). The resulting circuit is not always solved correctly by fixed-point iteration, but a simple bisection method gives correct solutions.

One aspect of the problem not addressed in this paper is the nature of the series impedance discussed in Section 4. The *Argon* software models this impedance explicitly in terms of types of footwear and paving surfaces. (For shocks other than via the feet, no series impedance appears to be allowed for.) The reduction of the geometry and materials of a given situation to a single series impedance value requires separate models beyond those we consider.

References

AS/NZS 60479.1 (2010). *Effects of current on human beings and livestock — general aspects* (cit. on p. M71).

Australia, Energy Networks. *Argon*. software accessed 11 March 2020 at https://www.energynetworks.com.au/resources/guidelines/industry-guidelines/ (cit. on pp. M67, M85).

Biegelmeier, G. (1960). "Ein Beitrag zur Problematik des Berührungsspannungsschutzes in Niederspannungsanlagen". In: *Elektrotechnische Zeitschrift B* 12, pp. 611–615 (cit. on p. M80).

Biegelmeier, G. (1979). "Über die Körperimpedanzen lebender Menschen bei Wechselstrom 50Hz". In: *Elektrotechnische Zeitschrift Archiv*, pp. 145–150 (cit. on p. M72).

— (1987). *Effects of current passing through the human body and the electrical impedance of the human body*. VDE-Verlag (cit. on p. M80).

Biegelmeier, G. and W.R. Lee (1980). "New considerations on the threshold of ventricular fibrillation for a.c. shocks at 50-60 Hz". In: *IEE Proceedings A* 127, pp. 103–110. DOI: 10.1049/ip-a-1.1980.0017 (cit. on p. M82).

Burden, R. L. and J. D. Faires (2001). *Numerical analysis*. 7th ed. Wadsworth (cit. on p. M79).

Dimopoulos, A. et al. (2012). "Proposal for probabilistic risk assessment in grounding systems and its application to transmission substations". In: *IEEE Transactions on Power Delivery* 27, pp. 2219–2226. DOI: 10.1109/TPWRD.2012.2204440 (cit. on p. M66).

Energy Networks Association (2010). *EG-0 Power system earthing guide*. Tech. rep. https://electrical-engineering-portal.com/download-center/books-and-guides/power-substations/power-system-earthing-guide (11 March 2020) (cit. on p. M82).

Ferris, L. P. et al. (1936). "Effects of electric shock on the heart". In: *Electrical engineering* 55, pp. 498–503. DOI: 10.1109/EE.1936.6539536 (cit. on p. M82).

Griffiths, I. and D. Woodhouse (2017). "A calculation framework for quantifying the probability of ventricular fibrillation of rare events". In: *IEEE Transactions on Power Delivery* 32, pp. 2052–2059. DOI: 10.1109/TPWRD.2016.2601306 (cit. on pp. M66, M72, M78, M83, M85).

Griffiths, I., D. Woodhouse, and S. Palmer (2013). "Use of finite probabilistic modelling to establish earthing hazard limits". In: IET Conference Publications. DOI: 10.1049/cp.2013.1270 (cit. on p. M82).

Hoffman, J. D. (2001). *Numerical methods for scientists and engineers*. 2nd ed. Marcel Dekker (cit. on p. M79).

International Electrotechnical Commission (2018). *IEC 60479-1:2018 Effects of current on human beings and livestock - Part 1: General aspects* (cit. on pp. M70, M71, M72, M77, M79, M80).

King, E. and R. Coggan (2016). "EG-0 constant fibrillation probability curve replication". In: Down to Earth conference. DOI: 10.1109/DTEC.2016.7731295 (cit. on p. M82).

Pawlik, B., I. Griffiths, and D. Woodhouse (2018). "Probability of coincidence: exposure to power system earth faults using Poisson patterns". In: Down to Earth conference. DOI: 10.1109/DTEC.2018.8726882 (cit. on p. M69).

Wang, W. et al. (1984). "A practical probabilistic method to evaluate tolerable step and touch voltages". In: *IEEE Transactions on Power Apparatus and Systems* PAS-103, pp. 3521–3530. DOI: DOI:10.1109/TPAS.1984.318382 (cit. on p. M66).

Author addresses

1. **G. Pritchard**, Dept. of Statistics, University of Auckland, New Zealand.
   mailto:g.pritchard@auckland.ac.nz
   orcid:0000-0002-5660-4503
2. **G. C. Livingston Jr**, School of Information and Physical Sciences, University of Newcastle, Australia.
   mailto:glen.livingstonjr@newcastle.edu.au
   orcid:0000-0002-9459-289X
3. **R. Aggarwal**, School of Information and Physical Sciences, University of Newcastle, Australia.
   orcid:0000-0003-4261-8223
4. **I. Griffiths**, Safearth Ltd., Australia.
5. **H. Waterer**, School of Information and Physical Sciences, University of Newcastle, Australia.
   orcid:0000-0002-5568-6252
6. **M. H. Meylan**, School of Information and Physical Sciences,

University of Newcastle, AUSTRALIA.
orcid:0000-0002-3164-1367

7. **J. Juniper**, Newcastle Business School, University of Newcastle, AUSTRALIA.
orcid:0000-0003-2973-6284